# Chitosan-based nanogels for selective delivery of photosensitizers to macrophages and improved retention in and therapy of articular joints

Frédéric Schmitt [a,1], Lucienne Lagopoulos [a,b,1], Peter Käuper [b], Nathanaël Rossi [b], Nathalie Busso [c], Jérôme Barge [d], Georges Wagnières [d], Carsten Laue [b], Christine Wandrey [e], Lucienne Juillerat-Jeanneret [a,*]

[a] *University Institute of Pathology, University of Lausanne (UNIL) and University Hospital (CHUV), Lausanne, Switzerland*
[b] *Medipol SA, Lausanne, Switzerland*
[c] *Département de l'Appareil Locomoteur, CHUV, Lausanne, Switzerland*
[d] *Medical Photonics Group, Institute of Chemical Sciences and Engineering, Swiss Federal Institute of Technology (EPFL), Lausanne, Switzerland*
[e] *Laboratoire de Médecine Régénérative et Phamacobiologie, Swiss Institutes of Technology (EPFL), Lausanne, Switzerland*

## ARTICLE INFO

## ABSTRACT

Macrophages play key roles in inflammatory disorders. Therefore, they are targets of treatments aiming at their local destruction in inflammation sites. However, injection of low molecular mass therapeutics, including photosensitizers, in inflamed joints results in their rapid efflux out of the joints, and poor therapeutic index. To improve selective uptake and increase retention of therapeutics in inflamed tissues, hydrophilic nanogels based on chitosan, of which surface was decorated with hyaluronate and which were loaded with one of three different anionic photosensitizers were developed. Optimal uptake of these functionalized nanogels by murine RAW 264.7 or human THP-1 macrophages as models was achieved after <4 h incubation, whereas only negligible uptake by murine fibroblasts used as control cells was observed. The uptake by cells and the intracellular localization of the photosensitizers, of the fluorescein-tagged chitosan and of the rhodamine-tagged hyaluronate were confirmed by fluorescence microscopy. Photodynamic experiments revealed good cell photocytotoxicity of the photosensitizers entrapped in the nanogels. In a mouse model of rheumatoid arthritis, injection of free photosensitizers resulted in their rapid clearance from the joints, while nanogel-encapsulated photosensitizers were retained in the inflamed joints over a longer period of time. The photodynamic treatment of the inflamed joints resulted in a reduction of inflammation comparable to a standard corticoid treatment. Thus, hyaluronate–chitosan nanogels encapsulating therapeutic agents are promising materials for the targeted delivery to macrophages and long-term retention of therapeutics in leaky inflamed articular joints.

## 1. Introduction

Recently developed approaches for the treatment of various diseases rely on encapsulation strategies to deliver therapeutic molecules to defined cells or tissues. These strategies involve either the covalent attachment of therapeutic agents to macromolecules or their entrapment by non-covalent interactions with the materials assembling into nanostructure. In both approaches, issues are to achieve defined localization of these nanodevices into living tissue and the controlled release from the nanodevices of the therapeutic agents in order to achieve therapeutic efficacy with minimal side effects. Macrophages are responsible of the increased vascular and tissue permeability observed at sites of inflammation, including in inflamed articular joints in pathologies such as rheumatoid arthritis [1–3], suggesting that their selective elimination may be beneficial for the treatment of inflammatory disorders. Thus, therapeutic protocols targeting macrophages may open new routes for the treatment of a wide range of diseases. Photodynamic therapy (PDT) is a modality of treatment already used in clinic for treating human diseases [4–7], including rheumatoid arthritis [8]. PDT involves a nontoxic photo-activable dye called a photosensitizer (PS) in combination with harmless visible light of defined wavelength, which excites the PS to a high energy triplet state. When excited, the PS reacts with cellular

oxygen to form toxic reactive oxygen species (ROS) such as singlet oxygen and oxygen radicals, which oxidize cellular nucleic, fatty and amino acids, and ultimately induce cell death. Several studies on animal models of rheumatoid arthritis using the photosensitizers photofrin, BPDMA, mTHPC or hexyl ester of 5-aminolevulinic acid have shown the benefit of PDT approaches [8–14]. However, one major problem of photodynamic therapy of inflamed tissues is the enhanced permeability resulting from inflammation and leakage of the therapeutics. This leakage could be avoided by the immobilization of the photosensitizers in a device that allows the photosensitizers to be targeted and retained in a defined body tissue. In this context, nanosized polymeric composites/carriers may be of interest. Several strategies involving nanosized carriers for photosensitizer delivery such as liposomes, polymeric micelles, metal-based or silica-based nanoparticles have already been explored [15–18]. The preparation of chitosan-based hydrophilic nanogels has been widely described in the literature, employing penta sodium triphosphate (PSTP) as the complexing anionic molecule for the polycation chitosan [19–25]. Chitosan-based nanogels have been studied as carriers of oligonucleotides in gene therapy, for mucosal vaccination, in tissue engineering or drug delivery [26–28]. However, highly positive nanoparticles are generally cytotoxic, or are unselectively taken up by cells due to their positive charge, suggesting that developing negative chitosan-based nanogels could be of biological interest. Nanogels based on a chitosan core matrix decorated on their surface with polyanions have been described [28,29].

We hypothesized that photosensitizers encapsulated in biocompatible polymers may reside longer in the joints and may achieve more efficient PDT. In addition, the encapsulation of photosensitizers in hyaluronate-decorated nanogels targeting macrophages would also improve selectivity of the process. In the present study, three different anionic photosensitizers, i.e. tetra-phenyl-porphyrin-tetra-sulfonate (TPPS$_4$), tetra-phenyl-chlorin-tetra-carboxylate (TPCC$_4$) and chlorin e6 (Ce6) (Fig. 1), were incorporated into hyaluronate-decorated chitosan-based nanogels.

These nanogels were studied as macrophage-targeting phototoxic materials for photodynamic therapy and in an in vivo study in mice using the antigen-induced arthritis (AIA) model of rheumatoid arthritis (RA) which recapitulates features of human RA.

## 2. Materials and methods

### 2.1. Nanogel formulation

Nanogels [30] were prepared by adding 10 mL of a 0.1% w/w penta sodium triphosphate solution (TPP, aka tripolyphosphate, Sigma-Aldrich, Steinheim, Germany) to 90 mL of a 0.1% w/w chitosan (low viscosity chitosan from Primex, Iceland, in-house purified by filtration through a 0.1 μm pore size hydrophilic filter (Minisart hydrophilic cellulose acetate, Sartorius, Germany)) or fluorescein-tagged (cf below) chitosan solution at pH 3.0 under constant stirring and by slow dropwise addition. The pH was maintained at pH 3.0 by adding 0.1 N HCl. The dispersion was stirred for 4 h and then stored overnight at 4 °C, followed by a filtration through a 1.2 μm pore size hydrophilic cellulose acetate filter (Minisart).

### 2.2. Incorporation of the photosensitizers TPPS$_4$, TPCC$_4$ or Ce6 into the nanogels

Water and 0.1 N HCl were added to the nanogel dispersion to obtain a 0.07% content of nanogels (dry residue) and a pH 3.0 formulation. The photosensitizers were dissolved in water at a concentration of 0.014% w/v for Ce6 (Frontier Scientific, Logan, UT, USA) and 0.018% w/v for TPCC$_4$ (Porphyrin Systems, Lübeck, Germany) and TPPS$_4$ (Sigma-Aldrich). The pH was adjusted to pH 7.0 and the solution was filtered through 0.2 μm microfilters (Minisart). Then,
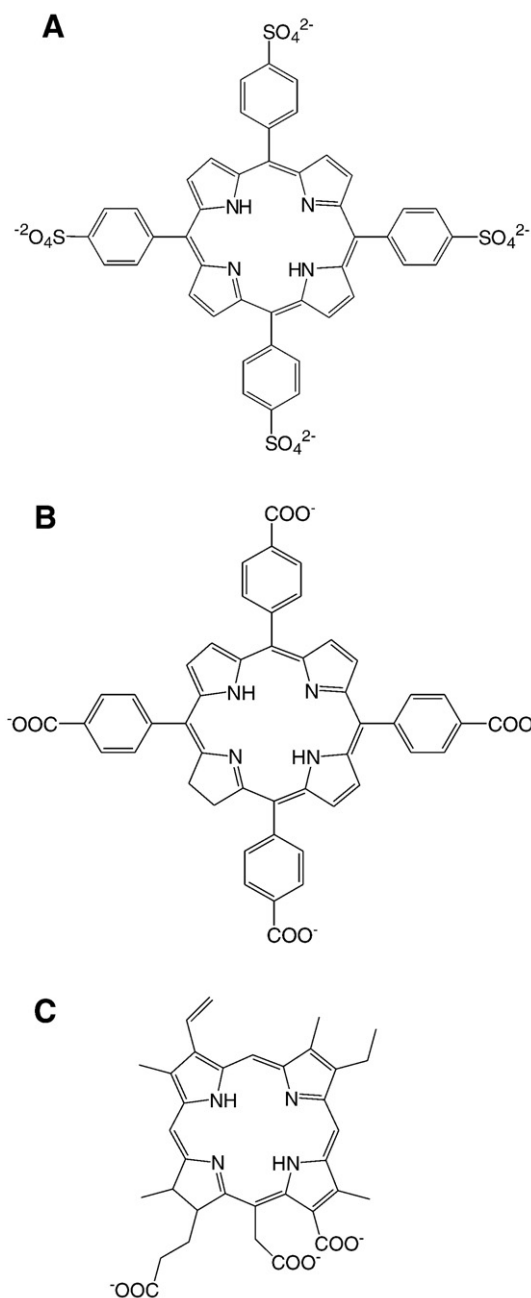


**Fig. 1.** *Chemical structures of the photosensitizers.* A. Tetra-phenyl-porphyrin-tetra-sulfonate (TPPS$_4$). B. Tetra-phenyl-chlorin-tetra-carboxylic acid (TPCC$_4$). C. Chlorin e6 (Ce6).

the photosensitizer solution was added slowly and drop-wise to the nanogel dispersion under constant stirring to obtain a final volume ratio of 1:1.75 volumes of nanogels formulation to photosensitizers. Stirring was continued for 2 h prior to the surface decoration process.

### 2.3. Surface decoration of the photensitizer-nanogels

Fifteen mL of either TPPS$_4$-, TPCC$_4$- or Ce6-nanogels were added drop-wise to 15 mL of a 0.05% w/w solution of hyaluronate (molar mass approx. 200,000 g/mol, Lifecore, Chaska, MN, USA) or rhodamine-tagged (cf below) hyaluronate under constant stirring. Then the pH was adjusted to 7.2 and stirring was continued for 2 h at room temperature. The dispersions were stored at 4 °C for at least 16 h before use. Prior to

application to cells, the dispersions were filtered through a 0.8 μm hydrophilic filter (Minisart) to remove aggregates and ensure a formulation of particles of approximately <1 μm in diameter.

## 2.4. Physical characterization of the nanogels

For scanning electron miscopy (SEM) the nanogels were filtered through a 30,000 g/mol Nanosep membrane (Pall, Basel, Switzerland). The filter membrane was dried at 37 °C followed by a platinum sputtering. The SEM images were obtained in a Zeiss Ultra 55 electron microscope at 2 kV (Zeiss, Oberkochen, Germany). The size distributions of the nanoparticles were determined from the SEM pictures. The surface charge of the nanogel formulations was analyzed by measuring the electrophoretic mobility in a Malvern Nanosizer (Malvern Ltd, Malvern, UK) and expressed as zeta potential. Surface-decorated nanogel dispersions were set to a pH of 7.4 and physiological NaCl concentration (0. 9% w/v) prior to measurements by mixing equivalent volumes of nanogel formulation and 1.8% w/w aqueous NaCl solution in 20 mM phosphate buffer pH 7.4, followed by filtration through a 0.8 μm hydrophilic filter (Minisart).

## 2.5. Preparation of the fluorescein-chitosan and rhodamine-hyaluronate nanogels

All chemicals were purchased from Sigma-Aldrich and used without further purification. Carboxyfluorescein was covalently bound to chitosan by an amide linkage between one of the chitosan amine functions and the carboxyfluorescein carboxylic acid function using carbodiimide chemistry. In detail, 5(6)-carboxyfluorescein was dispersed in water and 1% NaOH added until dissolution, then water was added to a final volume of 2 ml and a final concentration of 0.38%. To this solution, 1 mL of 3% sulfo-N-hydroxysuccinimide (sulfo-NHS) and of 0.4% EDC*HCl was added. After 25 min at room temperature, chitosan (3.45 mL, 1.16%) was added. The reaction mixture was stirred at room temperature overnight, then dialyzed (Spectra/Por Biotech Cellulose Ester Dialysis Membrane MWCO: 25,000 Spectrum Ls Europe B.V., Breda, The Netherlands) against demineralized water. The retentate was recovered by freeze drying and washed with acetone until no fluorescein absorbance could be recorded in the acetone.

N-Boc-ethylenediamine was first covalently bound to hyaluronate by an amide linkage between one of the hyaluronate carboxylic acid functions and the N-Boc-ethylenediamine amine function using carbodiimide chemistry. Then Rhodamine B isothiocyanate (RITC) was covalently linked via a thiourea linkage. In detail, sodium hyaluronate was dissolved at 3% in 2 mL water. To this solution 1 mL of 3% sulfo-NHS and of 0.29% EDC*HCl was added. After 25 min at room temperature, N-Boc-ethylenediamine (2.4 mg in 2 mL $H_2O$) was added. The reaction mixture was stirred at room temperature overnight, then dialyzed (Spectra/Por, MWCO: 100,000) against demineralized water. The retentate was recovered by freeze drying. To remove the Boc protecting group, trifluoroacetic acid (TFA) was added to the solid product and stirred for 40 min. TFA was then evaporated under a nitrogen stream and the product was freeze-dried. The solid was dissolved at 0.2% in 10 mL of a fresh 0.1 M carbonate buffer, pH 9. To this solution, 2 mL RITC solution in dimethyl sulfoxide (1.4 mg/mL) were added drop-wise. The reaction mixture was left at 4 °C overnight, then dialyzed (Spectra/Por MWCO: 100,000) against demineralized water. The retentate was recovered by freeze drying and washed with 2-propanol until no rhodamine absorbance could be recorded in 2-propanol.

## 2.6. Cells

The adherent RAW 264.7 murine macrophages, L929 and NIH-3T3 fibroblasts and non-adherent human THP-1 phagocytic macrophage-like monocytic leukemia cells were obtained from the ATCC (American Tissue Culture Collection, Manassas, Virginia, USA). All cell culture reagents were obtained from Gibco (Basel, Switzerland). RAW 264.7 and THP-1 macrophages were grown in DMEM medium containing 4.5 g/L glucose, 10% heat-inactivated fetal calf serum (FCS) and penicillin/streptomycin. L929 and NIH-3T3 fibroblasts were grown in DMEM medium containing 1 g/L glucose, 10% FCS and penicillin/streptomycin.

## 2.7. Determination of cytotoxicity

The RAW 264.7, L929 and NIH-3T3 cells were grown in 48-well cell culture plates (Corning, NY, USA) until 75% confluent. The culture media were replaced with fresh medium containing nanogels diluted in complete medium and the cells were exposed to the nanogels for 24 h. Then, medium was replaced with complete medium without nanogels and the cell viability was evaluated using the MTT assay, essentially as previously described [31]. Briefly, MTT (3-(4,5-dimethyl-2-thiazoyl)-2,5-diphenyltetrazolium bromide, Roche, Mannheim, Germany, 250 μg/mL final concentration) was added to the cells for 2 h, then the cell culture supernatants were removed, the cell layers were dissolved in 2-propanol/0.04 N HCl and absorbance at 540 nm was measured (iEMS Reader MF, Labsystems, Bioconcept, Switzerland) and compared to the values of control cells incubated without nanogels. Alternatively for non-adherent human THP-1 macrophages, the alamarBlue assay was performed, as previously described [31]. Briefly, cells were exposed to 10% Alamar Blue (Serotec, Düsseldorf, Germany) added to the cell culture medium and fluorescence increase was directly measured in a multiwell fluorescence reader ($\lambda_{ex}/\lambda_{em} = 530$ nm/580 nm) after 2 h at 37 °C.

## 2.8. Evaluation of cell uptake of Ce6-nanogels

Cells were grown in 48-well cell culture plates (Corning) until 75% confluent. The culture medium was replaced with fresh medium containing Ce6-nanogels diluted at 14% (v/v, final concentration) in complete medium and the cells were exposed to the nanogels for various periods of time. Then, the cells were washed with PBS and Ce6 fluorescence was measured in a thermostated fluorescence multiwell-plate reader (Cytofluor, PerSeptive BioSystems, Framingham, MA, USA), at $\lambda_{ex}/\lambda_{em} = 405/645$ nm, respectively. THP-1 cells were grown in 6-well cell culture plates (Corning) until reaching $10^6$ cell/mL. Then, 17% (v/v, final concentration) of Ce6-nanogel were added to cell medium and cells were exposed to the nanogels for various periods of time. Cells were centrifuged at 100 g for 5 min, washed with PBS and resuspended in 0.5 mL MeOH followed by ultra-sound treatment for 3 min. The suspension was centrifuged at 6000 g for 5 min and the Ce6 fluorescence of the supernatant was measured in a spectrofluorometer (LS50, PerkinElmer) at the Ce6-specific $\lambda_{ex}/\lambda_{em} = 409$ nm/645 nm, respectively.

## 2.9. Fluorescence microscopy

Cells were grown on histological slides in complete medium until 25% confluent and exposed to nanogels overnight in the dark. At the end of the incubation period, slides were washed in PBS and nuclei were stained with 4′,6′-diamidino-2-phenylindolylhydrochloride (DAPI, Roche Diagnostics) in PBS as previously described [32]. Then slides were mounted in PBS and analyzed, essentially as previously described [32], under a fluorescence microscope (Axioplan2, Carl Zeiss, Feldbach, Switzerland) with filters set at 365 ± 5 nm excitation light (BP 365/12, FT 395, LP 397) for DAPI, 470 ± 20 nm (BP 450–490, FT 510, BP 515–565) for carboxyfluorescein and 535 ± 25 nm excitation light (BP 510–560, FT 580, LP 590) for photosensitizers and rhodamine isothiocyanate.

## 2.10. Determination of nitric oxide (NO) production

Cell NO production was determined as nitrite accumulation in cell culture media using the Griess microassay, as previously described [33]. Briefly, 100 µL of cell supernatants was added to 100 µL of Griess reagent (0.5% w/w sulfanilamide and 0.05% w/w naphthylethylenediamine in 2.5% w/w phosphoric acid). Absorbance was measured at 540 nm in a multiwell-plate reader (iEMS Reader MF) and NO concentration was calculated by comparison with a standard sodium nitrite solution. Positive control of cell activation was obtained by incubating cells with γIFN (100 U/mL, Roche Diagnostics) and TNF-α (400 U/mL, Roche Diagnostics) under the same experimental conditions as the nanogels.

## 2.11. Determination of phototoxicity

Cells were grown in triplicate wells in 96-well cell culture plates (Corning) until 75% confluent. The culture media were replaced with fresh medium containing the PS-nanogels diluted at 17% (v/v, final concentration) in complete culture medium and the cells were exposed to the nanogels overnight. Then, the media were replaced with DMEM without phenol red containing 5% FCS and the cell layers were irradiated at 652 nm using a diode laser (Ceralas 652, Biolitec, Germany) coupled to a frontal diffuser (Medlight SA, Ecublens, Switzerland), at an irradiance of 20 mW/cm$^2$ and light doses from 0.5 to 15 J/cm$^2$, essentially as previously described [32,34]. Cell viability was evaluated 24 h later using the MTT assay. Values were compared to the values of control cells incubated without laser irradiation.

To determine the time-course of phototoxicity, cells were grown in 96-well cell culture plates (Corning) until 75% confluent. The culture medium was replaced with fresh medium containing PS-nanogels diluted at 17% or 8% v/v in complete medium and the cells were exposed to the PS-nanogels for up to 24 h. At defined times after PS-nanogel addition, the media were replaced with DMEM without phenol red containing 5% FCS and cells were irradiated at 652 nm with an irradiance of 20 mW/cm$^2$ and a light dose of 2 J/cm$^2$. Cell viability was evaluated 24 h later using the MTT assay. Values were compared to the values of control cells incubated without laser irradiation. THP-1 cells were grown in 6-well cell culture plates (Corning) until reaching 6.10$^5$ cell/mL. Then, 7% (v/v, final concentration) of Ce6-nanogel were added to the culture medium and the cells were incubated overnight. Then, the cell suspension was centrifuged at 100 g for 5 min, the cell pellets were resuspended in the same volume of medium without phenol red containing 5% FCS and the suspension was pipeted into triplicate wells of a 96-well plate (Corning) and irradiated at 652 nm with an irradiance of 20 mW/cm$^2$ and light doses up from 2 to 15 J/cm$^2$. Cell viability was evaluated using the alamarBlue assay. Briefly, 24 h after irradiation, Alamar Blue solution (10% final concentration, Serotec, Düsseldorf, Germany) was added to the cell culture medium without medium change and fluorescence increase was recorded 2 h later at 37 °C in a fluorescence microplate reader (Cytofluor, PerSeptive BioSystems) at $\lambda_{ex}/\lambda_{em} = 530$ nm/580 nm, respectively. Values were compared to the values of control cells incubated without laser irradiation.

## 2.12. Murine model of antigen-induced arthritis (AIA)

Male C57BL/6 mice were obtained from Charles River (L'Arbresle, France). All mice were housed under conventional conditions, and water and standard laboratory chow were provided ad libitum. All animal experiments were performed following International and National Animal Ethics guidelines and were approved by the Animal Ethics Committee of the Canton de Vaud, Switzerland (permit No 1876). AIA was induced essentially as previously described [35]. Briefly, 8 week-old anesthetized mice were immunized at days 0 and 7 by intradermal injection at the base of the tail of an emulsion of 100 µg methylated bovine serum albumin (mBSA) (Fluka, Buchs,

Switzerland) in 50 µL sterile PBS and 50 µL complete Freund's adjuvant mixed with 200 µg Mycobacterium tuberculosis (Difco Laboratories Inc., Franklin Lakes, NJ, USA). At day 0 mice were also injected intraperitoneally with 2.10$^9$ heat-killed Bordetella pertussis (Berna, Bern, Switzerland) in 0.5 mL serile PBS. At day 21, AIA was induced by intra-articular injection of 100 µg of mBSA in 10 µL sterile PBS into the joint of the right knee of mice, the left knee being injected with sterile PBS alone.

## 2.13. Evaluation of photosensitizer fluorescence in the knees of mice

At day 23, under anesthesia, a small cut in the skin of the knees was done in order to localize the site of injection of the nanogels in the small synovial cavity of the mice and 10 µL of either TPSS$_4$-nanogels were injected into the treated knees (right knee), or 10 µL of PBS in the control knees (left knee) of the same animal. The residual fluorescence of nanogels was evaluated at different times after injection using a detection fluorescence imaging system using a modified 300 W D-light source (Xe arc lamp from Storz, Tuttlingen, Germany) equipped with a red bandpass filter (635 nm, 20 nm FWHM; Chroma, USA), coupled to a Storz 4 mm diameter light guide. The output of this light guide was directed to the mice knee with a projection objective (Nikon, Japan; AF Nikkor; 1:1.4 D/50 mm) to generate a 2.5 cm diameter homogenous spot with an irradiance of 2 mW/cm$^2$ at 635 nm. The fluorescence was collected by another objective (Fujinon, Japan; TV zoom lens; 1:1.2/12.5–75 mm; Type H6X12.5R-MD3) through a longpass filter rejecting light below 665 nm (Schott, Germany; RG665) and the image was detected by a CCD camera (752×582 pixels CF 8/1 Kappa, Gleichen, Germany) equipped with an image intensifier (Proxifier BV 256-2FcZ-CH, Proxitronic, Bensheim, Germany). The images were captured by the 8-bits camera frame grabber and saved on the computer with the "Kappa Imagebase-control" software. Image treatment was carried out using the IPLab imaging software and the intensities of fluorescence were evaluated using the ImageJ software.

## 2.14. Photodynamic treatment of mice knees

At day 23, under anesthesia, the skin of the mice knees was cut open and injection of the Ce6-nanogel (10 µL/knee) was performed into the arthritic knee. Irradiation was performed 2.5 h later at 652 nm using a diode laser (Ceralas 652 from Biolitec, Bonn, Germany) coupled to a frontal diffuser (FD1 from Medlight, Ecublens, Switzerland), at an irradiance of 50 mW/cm$^2$ and increasing light doses from 3.3 to 25 J/cm$^2$. As controls for treatment efficacy two groups of mice were injected with either 25 µg of methylprednisolone acetate (Depo-medrol, Pfizer), a standard therapeutic agent for the treatment of RA in human patients, or PBS, respectively.

## 2.15. Evaluation of Serum Amyloid A (SAA)

Blood (0.2 mL) was taken from mice eight days after irradiation, centrifuged, stored as aliquots at −80 °C. Serum levels of SAA were determined using an ELISA assay (Biosource-Invitrogen, Camarillo, California) according to the manufacturer's protocol. Means ± sd were calculated.

## 2.16. Statistical analysis

Means ± standard deviation were calculated and Student's t-test was used for evaluation of statistical significance.

# 3. Results

In this study we define the nanogels as colloidal system of aggregates in the sub-micrometer range prepared from hydrophilic

**Table 1**
Zeta (ζ) potentials of the nanogels.

| Nanogel type | ζ potential [mV] |
| --- | --- |
| Ce6-nanogel | −48 |
| TPCC$_4$-nanogel | −39 |
| TPPS$_4$-nanogel | −41 |

polymers with gel-like characteristics and a size in the sub-micrometer range. Using the formulation of the chitosan–TPP–photosensitizer core as described resulted in nanogel preparation where only traces of uncomplexed chitosan and no detectable amount of photosensitizer were found in the dispersant, thus not requiring further purification. The encapsulation of the anionic photosensitizers (chemical structures shown in Fig. 1)) into hydrogels composed of chitosan and penta sodium triphosphate (PSTP) was based on electrostatic interaction yielding positively-charged photosensitizer-containing nanogels (PS–nanogels). To obtain negatively charged nanogels, the surface of the chitosan nanogels was decorated with hyaluronate. As expected, comparable negative ζ-potential values were obtained for all PS-nanogels (Table 1).

The size of the nanogels was estimated by scanning electron microscopy (SEM) of the dried nanogel dispersions. The determination of nanogel size by SEM under a dry state does not result in an accurate absolute value of the hydrated nanogel size in dispersion, but only visualizes size range and particle shape. The SEM picture of chlorine e6 (Ce6)-nanogels is shown in Fig. 2A. SEM analyses confirmed the relatively broad size distribution of the PS-nanogels,
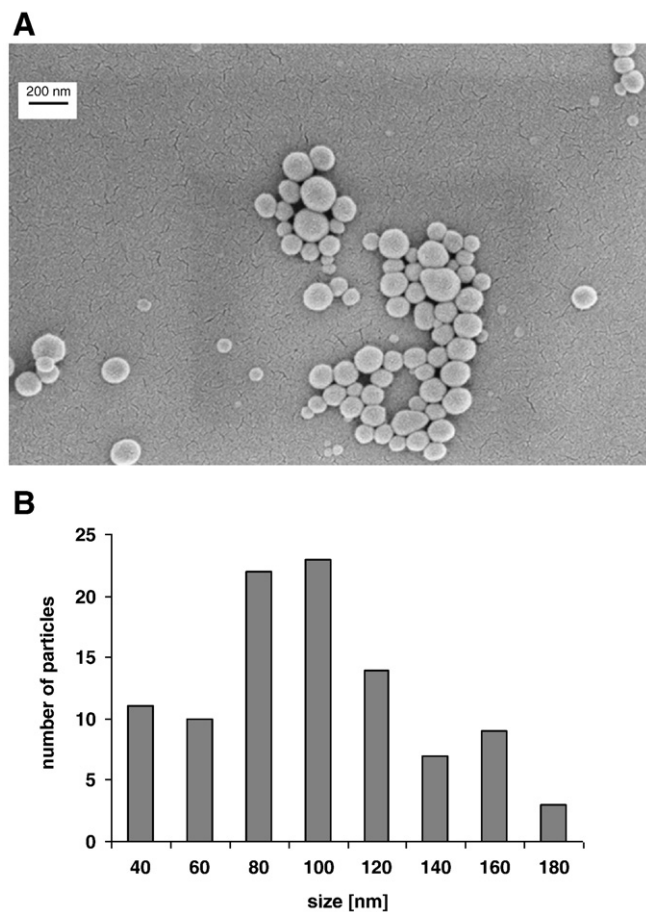
ranging from about 40 to 140 nm (Fig. 2B). The picture illustrates that the nanogel surface is smooth and regular.

The PS-nanogels were investigated *in vitro* as potential drug-delivery system for macrophages by evaluating their effect on the adherent murine RAW 264.7 and non-adherent human THP-1 macrophages. First, the cytotoxic potential of the three PS-nanogels in the absence of a photodynamic protocol was investigated in RAW 264.7 macrophages exposed for 24 h to increasing concentrations of PS-nanogels using a MTT cell survival assay (Fig. 3A). TPPS$_4$- and TPCC$_4$-nanogels were not cytotoxic in the dark at all concentrations tested while a cytotoxic effect appeared for Ce6-nanogels for a concentration >20%. For further experiments, a 17% concentration was chosen as the maximal concentration to avoid intrinsic cytotoxic effect of Ce6-nanogels. In human THP-1 macrophages, the increase in cell-associated fluorescence was a rapid event, and the maximal uptake was observed 3 h after addition of the PS-nanogels, followed by a phase of saturation of the uptake (Fig. 3B).

In order to determine whether exposure to these PS-nanogels may result in macrophage activation, the production of nitric oxide (NO) production, a very sensitive marker of activation of rodent macrophages [33], was determined. To control for RAW 264.7 macrophage responsiveness to activation, cells were exposed to γIFN and TNF-α [33]. Macrophage secretion of NO was evaluated after 24 h cell exposure to any of the three PS-nanogels (17%). None of the three PS-nanogels induced the production of NO by RAW 264.7 murine macrophages, whereas these cells responded to exposure to γIFN and TNF-α (Fig. 4).

Then the efficacy of PS-nanogels in photodynamic therapy protocols was determined. RAW 264.7 macrophages were exposed for 24 h to the PS-nanogels (17%), then to 652 nm light, with an irradiance of 20 mW/cm$^2$ and doses ranging from 0.5 to 15 J/cm$^2$ and cell survival was determined using the MTT assay 24 h after



**Fig. 2.** *Scanning electron microscopy (SEM) image of Ce6-hyaluronate-chitosan nanogels.* A. The Ce6-nanogel dispersion was filtered through a 30,000 g/mol filter, the filter was dried at 37 °C and platinum sputtering followed prior to SEM imaging. B. The size distribution of the Ce6-nanogels was determined from the SEM picture.
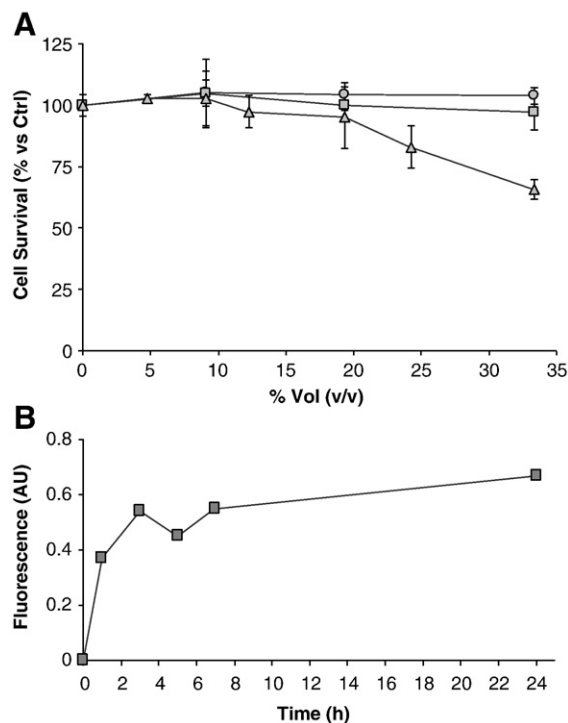


**Fig. 3.** *Interactions of Ce6-nanogels with macrophages.* A. Effect of PS-nanogel concentration on the survival of murine macrophages. RAW 264.7 macrophages were exposed for 24 h in the dark to PS-nanogels. RAW 264.7 cell survival was assessed using the MTT assay at the end of the incubation period. ○: TPCC$_4$-nanogels; ■: TPPS$_4$-nanogels; △: Ce6-nanogels. B. Time-dependent uptake of Ce6-nanogels by human THP-1 macrophages. Ce6-nanogels were diluted at 16% (v/v) in culture medium and added to THP-1 macrophages for increasing periods of time. Uptake was quantified by the Ce6-specific fluorescence.
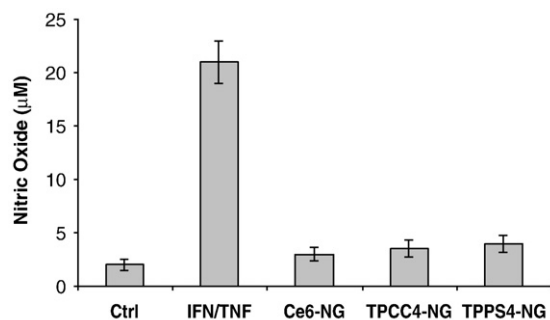
**Fig. 4.** *Nitric oxide (NO) production by murine macrophages exposed to PS-nanogels.* RAW 264.7 macrophages were exposed for 24 h to Ce6-, TPCC$_4$- or TPPS$_4$-nanogels (NG) diluted at 17% (v/v) in culture medium. The production of NO by cells activated with γIFN (100 U/mL) and TNF-α (400 U/mL) is shown for comparison.

completion of the irradiation (Fig. 5A). Cells treated with the same concentration of the PS-nanogels but kept in the dark were used as controls for dark toxicity, whereas cells which were not exposed to PS-nanogels but exposed to light were used as controls for laser light cytotoxicity. Untreated cells were not photosensitive in the absence of PS-nanogels, and PS-nanogels were not cytotoxic in the absence of light exposure. Phototoxicity responses for the three different PS-nanogels exhibited very different patterns of efficiency. For the Ce6-nanogels, the light dose which induced 50% of cell mortality (LD$_{50}$) was <0.5 J/cm$^2$, whereas the LD$_{50}$ in cells exposed to
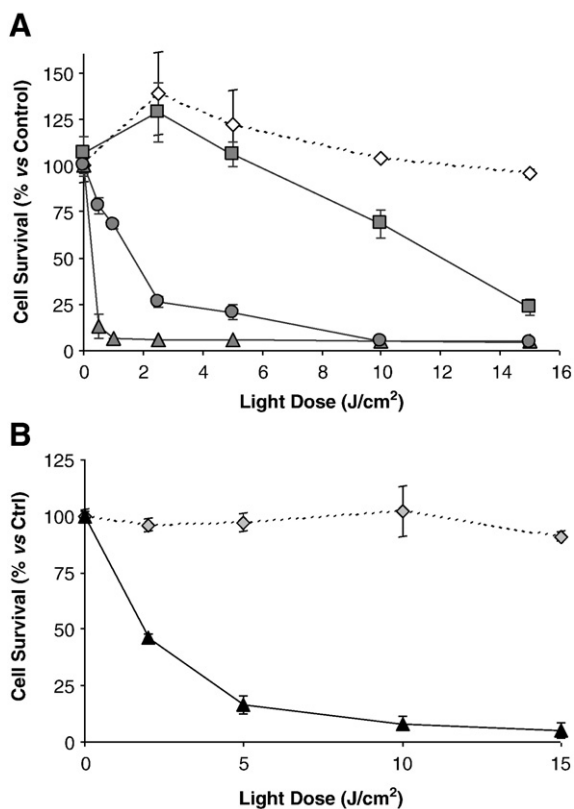


**Fig. 5.** *Photodynamic efficacy of PS-nanogels in RAW 264.7 murine and THP-1 human macrophages.* A. RAW 264.7 macrophages were exposed for 24 h to Ce6-, TPCC$_4$- or TPPS$_4$-nanogels diluted at 17% (v/v) in culture medium prior to irradiation by increasing doses of light at 652 nm. Cell survival was assessed 24 h later using the MTT assay. ◊: no nanogels; □: TPPS4-nanogels; △: Ce6-nanogels; ○: TPCC$_4$-nanogels. B. Human THP-1 macrophages were exposed for 24 h to Ce6-nanogels diluted at 7% (v/v) in culture medium prior to irradiation by increasing doses of light at 652 nm. Cell survival was assessed 24 h later using the alamarBlue assay. ▲: cells exposed to Ce6-nanogel; ◊: no nanogels.
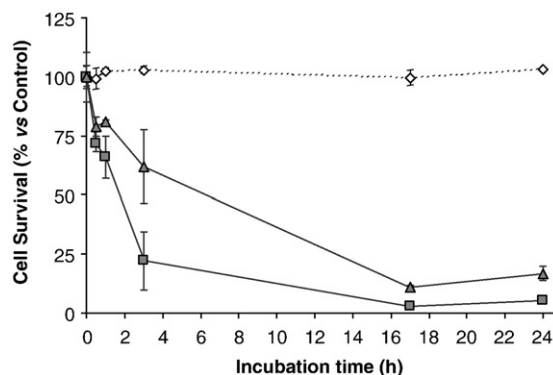


**Fig. 6.** *Time-dependent photodynamic efficacy of Ce6-nanogels in RAW 264.7 murine macrophages.* RAW 264.7 macrophages were exposed to Ce6-nanogels diluted at 8% or 17% (v/v) in culture medium for increasing incubation times and irradiated at 1 J/cm$^2$ dose of light at 652 nm and 20 mW/cm$^2$. Survival was assessed 24 h after irradiation using the MTT assay. ◊: no nanogels; △: 17% Ce6-nanogels; □: 8% Ce6-nanogels.

TPCC$_4$-nanogels or TPPS$_4$-nanogels were 2 J/cm$^2$ and 12 J/cm$^2$, respectively.

Human THP-1 macrophages were exposed to 7% Ce6-nanogels for 24 h, then exposed at 20 mW/cm$^2$ and light doses increasing from 2.5 to 15 J/cm$^2$. Cell survival was determined 24 h after the completion of the irradiation (Fig. 5B). THP-1 cells treated with the same concentration of the Ce6-nanogels but kept in the dark were used as controls for Ce6-nanogel dark toxicity. Untreated THP-1 macrophages were not photosensitive in the absence of PS-nanogels. For THP-1 macrophages exposed to Ce6-nanogels the LD$_{50}$ was ~2 J/cm$^2$. Cell irradiation in the absence of photosensitizer and/or nanogel demonstrated absence of cytotoxicity using the MTT test and PDT protocols performed in cells exposed to non-encapsulated photo-sensitizers demonstrated phototoxicity (results not shown).

Detailed time-course of phototoxic efficacy of Ce6-nanogels was performed on RAW 264.7 cells exposed to 2 different concentrations of Ce6-nanogels (8% and 17%) from 30 min to 24 h. At the end of the exposure period, cells were irradiated at 1 J/cm$^2$, culture was continued and the MTT survival assay was performed 24 h later. The phototoxic effect occurred very rapidly since efficacy was already apparent 30 min after cell exposure to the Ce6-nanogel. Less than 25% of cell survival was observed after 3 h of exposure to Ce6-nanogels (Fig. 6).

As control for macrophage selectivity, the time-dependent uptake of the Ce6-nanogels was monitored between 30 min and 24 h in RAW 264.7 murine macrophages and compared with L929 or NIH-3T3 murine fibroblasts (Fig. 7). The increase in cell-associated fluorescence in murine RAW 264.7 macrophages was a rapid event, and the maximal uptake was observed after 4 h of exposure, followed by
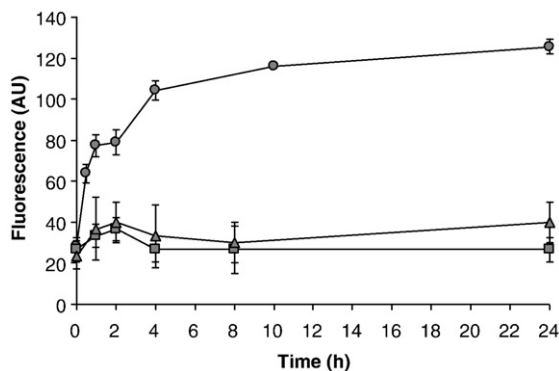


**Fig. 7.** *Time-dependent uptake of Ce6-nanogels by murine macrophages and fibroblasts.* Ce6-nanogels were diluted at 14% v/v in culture medium and added to RAW 264.7 macrophages, L929 or NIH-3T3 murine fibroblasts for increasing period of time. Uptake of Ce6 nanogels was quantified by the Ce6-specific fluorescence. ○: RAW 264.7 macrophages ; □: L929 fibroblasts; △: NIH- 3T3 fibroblasts.

saturation of the uptake, whereas in L929 and NIH-3T3 murine fibroblasts, no uptake of Ce6-nanogels was observed.

The uptake and intracellular localization of Ce6-nanogels in RAW 264.7 macrophages was confirmed by fluorescence microscopy (Fig. 8A), using the Ce6-associated red fluorescence as a reporter and DAPI labeling (blue) of the cell nuclei. The Ce6-associated fluorescence was found in the cell cytoplasm as red fluorescent spots. No nucleus-associated fluorescence was observed. Moreover,
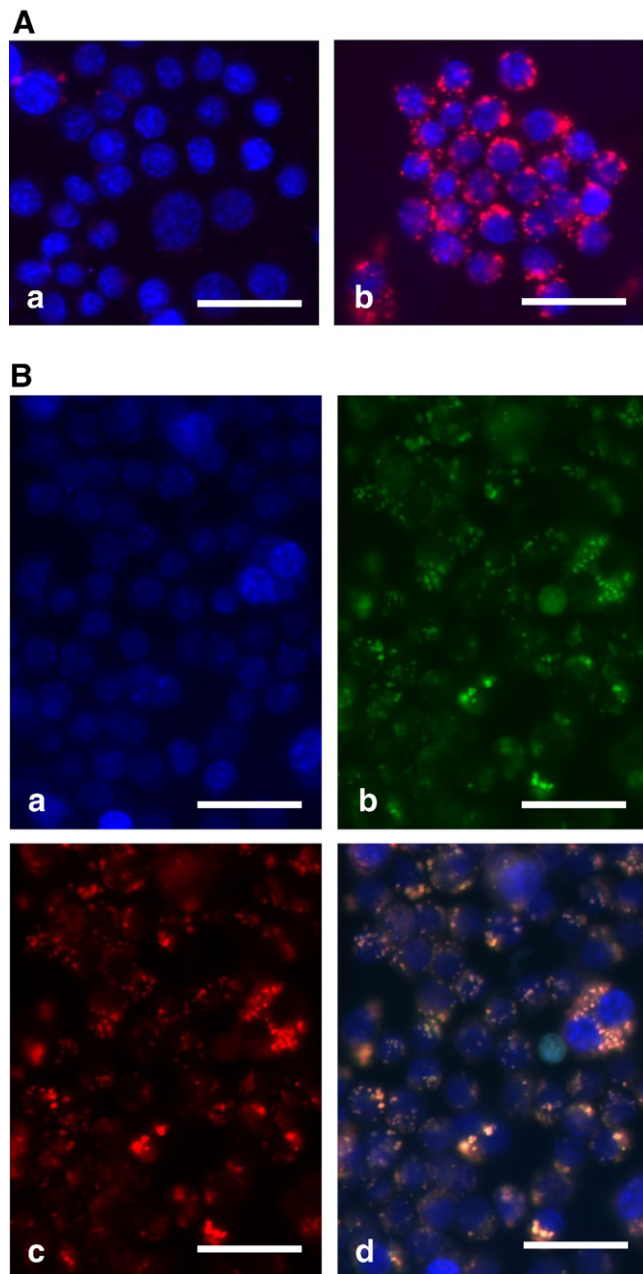
no nuclear fragmentation, a marker of cell apoptosis, was observed confirming the absence of cell toxicity in the absence of light exposure. Comparable information was obtained with TPPS$_4$- and TPCC$_4$-nanogels (results not shown). In order to determine whether the polymer components, chitosan and hyaluronate, forming the nanogels were also internalized by cells, chitosan was labeled with carboxyfluorescein (green fluorescence) and hyaluronate with rhodamine (red fluorescence) in nanogels not loaded with photosensitizer. RAW 264.7 macrophages were exposed to these PS-empty, fluorescence-tagged nanogels. The fluorescence associated to the two polymers was found co-localized in the cytoplasm of the cells (Fig. 8B). Again, no nuclear localization of the polymers was observed in the DAPI blue-fluorescent nuclei.

The photosensitizer-loaded nanogels were investigated *in vivo* as a potential photosensitizer delivery system for the photodynamic therapy of inflammatory diseases of articular joints using the murine model of antigen-induced arthritis (AIA). First, TPPS$_4$-nanogels were injected in normal mice knees and the clearance of the photosensitizer was evaluate by its associated fluorescence in the knees and compared to the clearance of free photosensitizer. The results showed that the fluorescence was retained much longer in the normal knees when the photosensitizer was injected as a nanogel compared to free photosensitizer (Fig. 9A). Then Ce6-nanogels were injected either in the normal knee or the arthritic knee of AIA mice. The Ce6-associated fluorescence was retained longer in arthritic knees compared to normal knees (Fig. 9B).

Then, the nanogels were evaluated in AIA mice as a potential photodynamic treatment for rheumatoid arthritis. Ce6-nanogels were injected in the arthritic knee of AIA mice and the knee was exposed 2 h
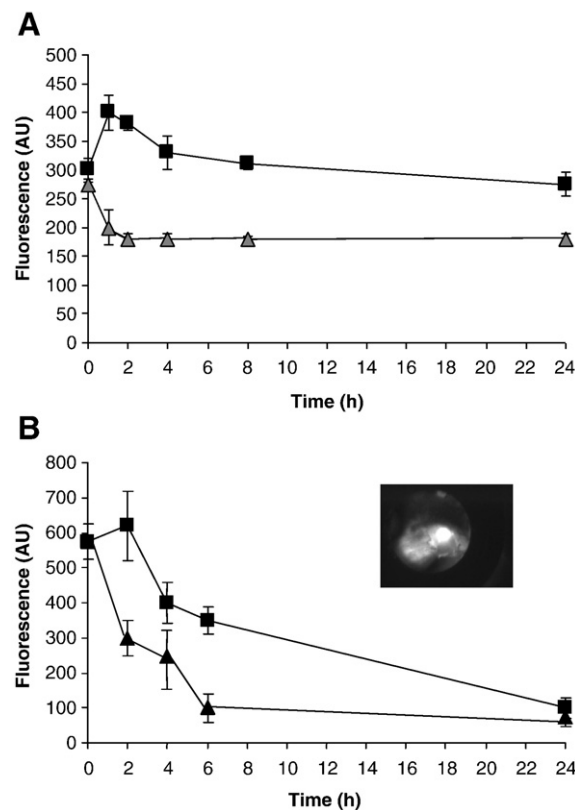


**Fig. 8.** *Intracellular accumulation of photosensitizer and nanogel polymers in murine macrophages.* A. RAW 264.7 macrophages were incubated overnight in the dark without (a) and with (b) Ce6-nanogels (15%, v/v) and nuclei were counterstained with DAPI. The cell uptake and localization of Ce6 and DAPI were analyzed by fluorescence microscopy. Ce6 and DAPI appear as red and blue fluorescence, respectively. B. Cells were incubated overnight in the dark with 15% (v/v) nanogels composed of carboxyfluorescein-chitosan (CF) and rhodamine isothiocyanate-hyaluronate (RITC). Nuclei were counterstained with DAPI. The cell uptake and localization of DAPI, CF and RITC were analyzed by fluorescence microscopy. Fluorescence images of DAPI, CF and RITC are respectively represented in a, b, c while the merged images are shown in d. Scale bars represent 20 μm in all pictures.



**Fig. 9.** *Retention of photosensitizers in mice knees as free drugs or as nanogels.* A. Fluorescence of the TPPS$_4$ photosensitizer injected in normal mice knee. TPPS$_4$ was injected in the mice knees as TPPS$_4$-nanogels (■) or as free molecule (△). B. Fluorescence of the Ce6-nanogels injected in mice knee. Ce6 nanogels were injected in normal (△) or arthritic knee from AIA mice (■). *Insert.* Representative Ce6 fluorescence image 1 h after injection of Ce6-nanogels in arthritic knee.
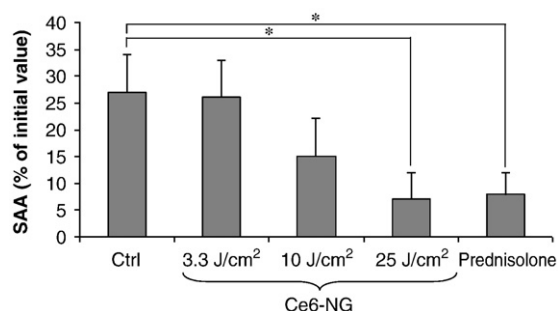
**Fig. 10.** *Serum Amyloid A (SAA) levels.* Circulating levels of SAA were determined eight days after injection in the mice knees (number of mice $\geq 7$) of either Ce6-nanogels (Ce6-NG) or methylprednisolone and photodynamic treatment protocol. An unpaired Student's *t*-test was used for evaluation of statistical significance. For each group, $n \geq 7$. *: $p > 0.05$.

and 30 min later to light at 652 nm with an irradiance of 50 mW/cm$^2$ with light doses from 3.3 to 25 J/cm$^2$. Eight days after irradiation, blood samples were taken from treated mice and the serum levels of Serum Amyloid A (SAA), an acute-phase protein, was quantified as reporter of inflammation (Fig. 10). Results showed that the SAA levels decreased strongly after the treatment at 25 J/cm$^2$, reaching values comparable to the values measured after the injection of prednisolone, a standard corticoid treatment used in clinic for the treatment of rheumatoid joints.

## 4. Discussion

In the study presented here, chitosan-based nanogels whose surface was decorated with hyaluronate and incorporating amphiphilic photoactive molecules were prepared. The formation of the nanogels composed of chitosan, penta sodium triphosphate and one anionic photosensitizer was primarily based on electrostatic interactions yielding hydrogels. The tetrapyrolic ring and the side chains bearing carboxylate or sulfonate moieties of the photosenzitizers chosen allowed their entrapment into the positively-charged chitosan core of the nanogels. The advantages of decorating the nanogels with hyaluronate were multiple: the positive charge of chitosan is inverted to negative charge, thus favouring biocompatibility, hyaluronate has the potential to target the CD44 cell surface receptor of macrophages which is involved in phagocytosis [36,37] and is overexpressed in the activated macrophages. Thus hyaluronate decoration of nanogels improved both selectivity and uptake of nanogels by the macrophages. Moreover, as intraarticular injection of hyaluronate has beneficial effects in patients with rheumatoid arthritis [38], the presence of hyaluronate at the surface of the nanogels in inflamed joints will not further enhance inflammation.

Using murine and human macrophages we demonstrated that these chitosan-based nanogels can deliver photosensitizers to macrophages, then allowing effective PDT protocols to be performed. Murine fibroblasts used as control cells of a non-macrophage origin did not take up these PS-nanogels. In an arthritic knee, many cells including immune cells and synoviocytes are activated/stimulated by bacterial products and cytokines. Under these conditions, synoviocytes would behave in part as macrophages. We used fibroblasts not as a model for activated/stimulated synoviocytes, but as a model of non-activated cells, to determine whether this type of resting cells would also be affected by the PS-nanogels, and exclude generalized inflammatory or unspecific effects of the PS-nanogels. The polymers used to form the nanogels are known as biocompatible [26]. In agreement with this information, we did not observe any cytotoxicity in the absence of light exposure, even at very high level of cell exposure to the PS-nanogels. Only the Ce6-nanogels were slightly cytotoxic at high concentration, due to the known intrinsic cytotoxicity of this photosensitizer. The cell uptake of such PS-nanogels was

very rapid ($<4$ h) and the fluorescence associated with the photosensitizer was retained inside cells for up to 24 h. Fluorescence microscopy studies demonstrated that the photosensitizer and the two polymers forming the nanogels were taken up by the macrophages and concentrated in cell cytoplasm and organelles, but not in the nucleus. A delivery system, which targets inflammatory diseases, must not over-activate the target cells. NO is a key factor secreted at high levels by activated rodent macrophages. The demonstrated absence of secretion of NO by murine macrophages incubated with the PS-nanogels confirmed this important property of the nanogels. Comparable information had been previously obtained using other types of nanoparticles, including dextran-coated ultrasmall superparamagnetic iron oxide (USPIO) nanoparticles used in clinics as MRI contrast agents [39].

Singlet oxygen, which is the cytotoxic entity formed during the photodynamic treatment, is produced in very close proximity of the photosensitizer and has a very short half-life in aqueous media. Therefore, achieving intracellular uptake of photosensitizers is necessary for good phototoxic efficacy. The photosensitizer encapsulated in the nanogels achieved good photodynamic efficiency displaying LD$_{50}$ values comprised between $<0.5$ J/cm$^2$, 2 J/cm$^2$ or 12 J/cm$^2$, respectively, dependent on the particular photosensitizer. As no significant differences in the uptake of the three PS-nanogels by macrophages were observed, these results are compatible with the known hierarchy of intrinsic photodynamic efficiencies of the three photosensitizers. It has to be noted that light doses of 1–15 J/cm$^2$ and up to 48 J/cm$^2$ are generally used in most photodynamic therapy protocols [33,34,40–43].

The antigen-induced arthritis (AIA) model of rheumatoid arthritis (RA) recapitulates features of human RA [44,45]. This model is based on a T cell-mediated joint inflammation. PDT protocols have been previously evaluated in models of RA [8–12], using various photosensitizers in several animal models of AIA. The photosensitizers BPDMA, mTHPC or 5-aminolevulinic acid hexyl ester were also evaluated in murine models of AIA with beneficial effects [10–12]. In our approach, the efficiency of photodynamic treatment of mice knees was evaluated by measuring the concentration in mice blood of the Serum Amyloid A (SAA), an acute-phase protein which is used in the diagnosis and prognosis of human adult RA and AIA models [13,14,45,46]. SAA measurements in the blood, when compared to histological examination of slides of the knees at the end of the experimental period, allow to follow the time-course of response to treatment. In addition, SAA measurement allows to obtain more objective and quantitative information than grading of histological slides.

The quantification, eight days after light exposure, of the circulating levels of SAA demonstrated the efficiency of the PDT treatment at 25 J/cm$^2$. With this PDT protocol, SAA levels after this PDT protocol were comparable with the SAA levels obtained after intraarticular injection of methylprednisolone, a corticoid used in the clinic for the local treatment of RA patients.

## 5. Conclusion

In conclusion, the present results demonstrated that hydrophilic chitosan-based nanogels decorated with hyaluronate and encapsulating photosensitizers are excellent drug-delivery systems for the selective delivery of photosensitizers to macrophages and photodynamic destruction of these cells. This nanogel delivery system was also efficient *in vivo* for increasing the retention and decreasing the clearance of photosensitizers from the inflamed leaky articular joints in a murine modeld of rheumatoid arthritis, This nanogel system also allowed efficient PDT protocols to be performed *in vivo*. Therefore benefit can be expected in using such a delivery system to treat inflamed articular joint not only for photosensitizers and PDT protocols, but also for other chemotherapeutics.

**NANOMEDICINE**

## References

[1] N. Fujiwara, K. Kobayashi, Macrophages in inflammation, Curr. Drug Targets 4 (2005) 281–286.

[2] M. Feldmann, Development of anti-TNF therapy for rheumatoid arthritis, Nat. Rev., Immunol. 5 (2002) 364–371.

[3] Y. Ma, R.M. Pope, The role of macrophages in rheumatoid arthritis, Curr. Pharm. Des. 11 (2005) 569–580.

[4] S.B. Brown, E.A. Brown, I. Walker, The present and future role of photodynamic therapy in cancer treatment, Lancet Oncol. 5 (2004) 497–508.

[5] D.E. Dolmans, D. Fukumura, R.K. Jain, Photodynamic therapy for cancer, Nat. Rev., Cancer 3 (2003) 380–387.

[6] E.S. Nyman, P.H. Hynninen, Research advances in the use of tetrapyrrolic photosensitizers for photodynamic therapy, J. Photochem. Photobiol., B (2004) 1–28.

[7] Y.G. Qiang, X.P. Zhang, J. Li, Z. Huang, Photodynamic therapy for malignant and non-malignant diseases: clinical investigation and application, Chin. Med. J. 119 (2006) 845–857.

[8] K. Trauner, R. Gandour-Edwards, M. Bamberg, N.S. Nishioka, T. Flotte, S. Autry, T. Hasan, Influence of light delivery on photodynamic synovectomy in an antigen-induced arthritis model for rheumatoid arthritis, Laser Surg. Med. 22 (1998) 147–156.

[9] L.G. Ratkay, R.K. Chowdhary, A. Iamaroon, A.M. Richter, H.C. Neyndorff, E.C. Keystone, J.D. Waterfield, J.G. Levy JG, Amelioration of AIA in rabbits by induction of apoptosis of inflammatory cells with local application of transdermal photodynamic therapy, Arthritis Rheum. 3 (1998) 525–534.

[10] C. Hendrich, G. Huttmann, J.L. Vispo-Seara, S. Houserek, W.E. Siebert, Experimental photodynamic laser therapy for rheumatoid arthritis with a second generation photosensitizer, Knee Surg. Sports Traumatol. Arthrosc. 8 (2000) 190–194.

[11] A. Hansch, O. Frey, M. Gadja, G. Susanna, J. Boettcher, R. Brauer, W. Kaiser, Photodynamic treatment as a novel approach in the therapy of arthritis joints, Laser Surg. Med. 40 (2008) 265–272.

[12] G. Kirdaite, N. Lange, N. Busso, H. van den Bergh, P. Kucera, A. So, Protoporphyrin IX photodynamic therapy for synovitis, Arthritis Rheum. 5 (2002) 1371–1378.

[13] B. Funke, A. Jungel, S. Schaslak, K. Wiedemeyer, F. Emmrich, U. Sack, Transdermal photodynamic therapy — a treatment option for rheumatic destruction of small joints, Laser Surg. Med. 38 (2006) 866–874.

[14] S. Urieli–Shoval, R.P. Linke, Y. Matzner, Expression and function of serum amyloid A, a major acute–phase protien, in normal and disease states, Curr. Opin. Hematol. 7 (2000) 64–69.

[15] A.S.L. Derycke, P.A.M. deWitte, Liposomes for photodynamic therapy, Adv. Drug Deliv. Rev. 56 (2004) 17–30.

[16] C.F. van Nostrum, Polymeric micelles to deliver photosensitizer for photodynamic therapy, Adv. Drug Deliv. Rev. 56 (2004) 9–16.

[17] M. Regehly, K. Greish, F. Rancan, H. Maeda, F. Bohm, B. Roder, Water-soluble polymer conjugates of ZnPP for photodynamic tumor therapy, Bioconj. Chem. 18 (2007) 494–499.

[18] I. Roy, T.Y. Ohulchanskyy, H.E. Pudavar, E.J. Bergey, A.R. Oseroff, J. Morgan, T.J. Dougherty, P.N. Prasad, Ceramic-based nanoparticles entrapping water-insoluble photosensitizing anticancer drugs: a novel drug carrier system for photodynamic therapy, J. Am. Chem. Soc. 125 (2003) 7860–7865.

[19] P. Calvo, C. Remunan-Lopez, J.L. Vila-Jato, Novel hydrophilic chitosan–polyethylene oxide nanoparticles as protein carriers, J. Appl. Polym. Sci. 63 (1997) 125–132.

[20] R. Fernandez-Urrusuno, P. Calvo, C. Remunan-Lopez, J.L. Vila-Jato, M.J. Alonso, Enhancement of nasal absorption of insulin using chitosan nanoparticles, Pharm. Res. 16 (1999) 1576–1581.

[21] K.A. Janes, P. Calvo, M.J. Alonso, Polysaccharide colloidal particles as delivery systems for macromolecules, Adv. Drug Deliv. Rev. 47 (2001) 83–97.

[22] A. Vila, A. Sanchez, K.A. Janes, I. Behrens, T. Kissel, J.L. Vila Jato, M.J. Alonso, Low molecular weight chitosan nanoparticles as new carriers for nasal vaccine delivery in mice, Eur. J. Pharm. Biopharm. 57 (2004) 123–131.

[23] Y. Aktas, K. Andrieux, M.J. Alonso, P. Calvo, R.N. Gürsoy, P. Couvreur, Y. Capan, Preparation and in vitro evaluation of chitosan nanoparticles containing a caspase inhibitor, Int. J. Pharm. 298 (2005) 378–383.

[24] Q. Gan, T. Wang, C. Cochrane, P. McCarron, Modulation of surface charge, particle size and morphological properties of chitosan–TPP nanoparticles intended for gene delivery, Colloids Surf., B Biointerfaces 44 (2005) 65–73.

[25] Q. Gan, T. Wang, Chitosan nanoparticle as protein delivery carrier — systematic examination of fabrication conditions for efficient loading and release, Colloids Surf., B Biointerfaces 59 (2007) 24–34.

[26] J.M. Dang, K.W. Leong, Natural polymers for gene delivery and tissue engineering, Adv. Drug Deliv. Rev. 58 (2006) 487–499.

[27] S.A. Agnihotri, N.N. Mallikarjuna, T.M. Aminabhavi, Recent advances on chitosan-based micro- and nanoparticles in drug delivery, J. Control. Release 100 (2004) 5–28.

[28] O. Borges, A. Cordeiro-da-Silva, S.G. Romeijn, M. Amidi, A. de Sousa, G. Borchard, H.E. Junginger, Uptake studies in rat Peyer's patches, cytotoxicity and release studies of alginate coated chitosan nanoparticles for mucosal vaccination, J. Control. Release 114 (2006) 348–358.

[29] O. Borges, G. Borchard, J.C. Verhoef, A. de Sousa, H.E. Junginger, Preparation of coated nanoparticles for a new mucosal vaccine delivery system, Int. J. Pharm. 299 (2005) 155–166.

[30] Hynospheres patent: US61/007, 690, Colloidal particle comprising multivalent cyclic anions, 12/14/2007.

[31] F. Cengelli, J.A. Grzyb, A. Montoro, H. Hofmann, S. Hanessian, L. Juillerat-Jeanneret, Surface-functionalized ultrasmall superparamagnetic nanoparticles as magnetic delivery vectors for camptothecin, Chem. Med. Chem. 4 (2009) 988–997.

[32] F. Schmitt, P. Govindaswamy, G. Süss-Fink, W.H. Ang, P.J. Dyson, L. Juillerat-Jeanneret, B. Therrien, Ruthenium porphyrin compounds for photodynamic therapy of cancer, J. Med. Chem. 51 (2008) 1811–1816.

[33] S. Lohm, L. Peduto-Eberl, P. Lagadec, N. Renggli-Zulliger, J. Dudler, J.F. Jeannin, L. Juillerat-Jeanneret, Evaluation of the interaction between TGF beta and nitric oxide in the mechanisms of progression of colon carcinoma, Clin. Exp. Metastasis 22 (2005) 341–349.

[34] F. Schmitt, P. Govindaswamy, O. Zava, G. Süss-Fink, L. Juillerat-Jeanneret, B. Therrien, Combined arene ruthenium porphyrins as chemotherapeutics and photosensitizers for cancer therapy, J. Biol. Inorg. Chem. 14 (2009) 101–109.

[35] D. Brackertz, G.F. Mitchell, I.R. Mackay, Antigen induced arthritis in mice. I. Induction of arthritis in various strains of mice, Arthritis Rheum. 20 (1977) 841–850.

[36] D. Naor, S. Nedvetzki, CD44 in rheumatoid arthritis, Arthritis Res. Ther. 5 (2003) 105–115.

[37] E. Vachon, R. Martin, J. Plumb, V. Kwok, W. Vandivier, M. Glogauer, A. Kapus, X. Wang, C.W. Chow, S. Grinstein, G.P. Downey, CD44 is a phagocytic receptor, Blood 107 (2006) 4149–4158.

[38] S. Saito, S. Kotake, Is there evidence in support of the use of intra-articular hyaluronate in treating rheumatoid arthritis of the knee ? A meta-analysis of the published litteratue, Modern Rheumatol. 19 (2009) 493–501.

[39] F. Cengelli, D. Maysinger, F. Tschudi-Monnet, X. Montet, C. Corot, A. Petri-Fink, H. Hofmann, L. Juillerat-Jeanneret, Interaction of functionalized superparamagnetic iron oxide nanoparticles with brain structures, J. Pharmacol. Exp. Ther. 318 (2006) 108–116.

[40] L. Cohen, S. Schwartz, Modification of radiosensitivity by porphyrins: II. Transplanted rhabdomyosarcoma in mice, Cancer Res. 26 (1966) 1769–1773.

[41] A.J. Barrrett, J.C. Kennedy, R.A. Jones, P. Nadeau, R.H. Pottier, The effect of tissue and cellular pH on the selective biodistribution of porphyrin-type photochemotherapeutic agents: a volumetric titration study, J. Photochem. Photobiol., B 6 (1990) 309–323.

[42] S. Fickweiler, R.M. Szeimies, W. Baumler, P. Steinbach, S. Karrer, A.E. Goetz, C. Abels, F. Hofstadter, M. Landthaler, Indocyanine green: intracellular uptake and phototherapeutic effects in vitro, J. Photochem. Photobiol., B 38 (1997) 178–183.

[43] R. Schneider, F. Schmitt, C. Frochot, Y. Fort, N. Lourette, F. Guillemin, J.F. Muller, M. Barberi-Heyob, Design, synthesis, and biological evaluation of folic acid targeted tetraphenylporphyrin as novel photosensitizers for selective photodynamic therapy, Bioorg. Med. Chem. 13 (2005) 2799–2808.

[44] J. Simon, R. Surber, G. Kleinstauber, P.K. Petrow, S. Henzgen, R.W. Kinne, R. Brauer, Systemic macrophage activation in locally-induced experimental arthritis, J. Autoimmun. 17 (2001) 127–136.

[45] G. Palmer, N. Busso, M. Aurrand-Lions, D. Tabalot-Ayer, V. Chobaz-Peclat, C. Zimmerli, P. Hammel, B.A. Imhof, C. Gabay, Expression and function of junctional adhesion molecule C in human and experimental arthritis, Arthritis Res. Ther. 9 (2007) R65.

[46] J. Marcinkiewicz, P. Gluszko, E. Kontny, B. Kwasny-Krochin, B. Bobek, W. Wierzchowski, M. Ciszek, W. Maslinski, Is taurolidine a candidate for treatment of rheumatoid arthritis? Clin. Exp. Rheumatol. 25 (2007) 211–218.